

Interacting dimers on the honeycomb lattice: An exact solution of the five-vertex model

H. Y. Huang and F. Y. Wu
Department of Physics
Northeastern University
Boston, Massachusetts 02115

H. Kunz
Institut de Physique Théorique
Ecole Polytechnique Fédérale
Lausanne, Switzerland

D. Kim
Center for Theoretical Physics
Seoul National University
Seoul, Korea 151-742

Abstract

The problem of close-packed dimers on the honeycomb lattice was solved by Kasteleyn in 1963. Here we extend the solution to include interactions between neighboring dimers in two spatial lattice directions. The solution is obtained by using the method of Bethe ansatz and by converting the dimer problem into a five-vertex problem. The complete phase diagram is obtained and it is found that a new frozen phase, in which the attracting dimers prevail, arises when the interaction is attractive. For repulsive dimer interactions a new first-order line separating two frozen phases occurs. The transitions are continuous and the critical behavior in the disorder regime is found to be the same as in the case of noninteracting dimers characterized by a specific heat exponent $\alpha = 1/2$.

1 Introduction

An important milestone of the modern theory of lattice statistics is the exact solution of the dimer problem obtained by Kasteleyn [1] and by Fisher [2]. Kasteleyn and Fisher considered the problem of close-packed dimers on the simple quartic lattice and succeeded in evaluating its generating function in a closed-form expression. While the solution shows that close-packed dimers on the square lattice do not exhibit a phase transition, Kasteleyn [3] later pointed out that dimers on the honeycomb lattice do possess phase changes, and that the transitions are accompanied by frozen ordered states. The solution, which has since been analyzed by one of us [4, 5], can be used to describe domain walls in two dimensions [6, 7].

In this paper we consider once again close-packed dimers on the honeycomb lattice, but now with the introduction of interactions between neighboring dimers along two lattice directions. We show that, with the onset of dimer-dimer interactions, a new ordered phase emerges if the interaction is attractive. For repulsive interactions the phase diagram is drastically changed and a tricritical point emerges. We deduce locations of all phase boundaries and study its critical behavior.

We analyze interacting dimers by first converting the problem into a five-vertex model. For noninteracting dimers this leads to a free-fermion model [8] which can be solved by using the method of Pfaffians [1, 4, 5]. But when interactions are present the five-vertex model has general vertex weights and the method of Pfaffians is no longer applicable. While its solution is in principle obtainable from that of the six-vertex model by Sutherland, Yang and Yang announced in [9], but details of [9] has not yet been published. Likewise, recently published analyses of the general six-vertex model in the regime $\Delta < 1$ by Nolden [10] and in the regime $\Delta \geq 1$ by Bukman and Shore [11, 12], where Δ is a parameter occurring in the six-vertex model, do not readily translate into the five-vertex problem since the five-vertex model corresponds to taking the $|\Delta| \rightarrow \infty$ limit. In fact, it is precisely because of this special situation that the analysis of the five-vertex model as a limit of the six-vertex model requires special care. To be sure, several authors [7, 13] have recently studied the five-vertex model. But the five-vertex model considered in [13] is confined to a special regime of the parameter space which does not yield the complete complexity of the system. The treatment in [7], which was aimed to studying domain walls, is more complete but analyzes the Bethe ansatz solution along a line somewhat different from

what we shall present, and is not transparent in extracting relevant information on the dimer system. It is therefore useful to have an alternate and self-contained analysis of the five-vertex model in the language of dimer statistics.

We take up this subject matter in the present paper. Our approach is essentially that of [9], by considering the solution of the Bethe ansatz equations in the complex plane. However, we follow the Bethe ansatz solutions closely and explicitly carry out all relevant contour integrations as dictated by relevant physical considerations. This leads to a complete and clear picture of the phase diagram and critical behavior of the interacting dimer system. Particularly, we find the emergence of a new ordered phase for attractive dimer-dimer interactions, and the existence of a first-order line terminating at a new kind of tricritical point, when the interactions are repulsive.

The organization of our paper is as follows. The problem of interacting dimers is defined in section 1 and mapped into a five-vertex model in section 2. The Bethe ansatz equation is set up in section 3, and solved in section 4 in the case of noninteracting dimers. In section 5 we analyze the general Bethe ansatz equation, obtaining expressions for the free energy and its derivative. This leads to the determination of the contour of integrations in section 6 and the complete phase diagram in section 7. Finally, the critical behavior is determined in section 8 by applying perturbation calculations to the free energy.

2 The five-vertex model

Consider close-packed dimers on an honeycomb lattice \mathcal{L} which we draw as a “brick-wall” shown in Fig. 1. To each dimer along the three edges incident at a vertex, one associates a fugacity, or weight, u, v , or w . A vertical u dimer and a horizontal v dimer are said to be neighbors if they happen to occupy two neighboring sites in the same row. Let two neighboring u and v dimers interact with an energy $-\epsilon$ and thus possessing a Boltzmann factor

$$\sqrt{\lambda} = e^{\epsilon/kT}, \quad (2.1)$$

with $\lambda > 1$ ($\lambda < 1$) denoting attractive (repulsive) interactions. Other pairs of dimers such as u - u , u - w etc. are not interacting in our model. Then, by replacing the two sites inside each dotted box containing a w -edge in Fig. 1 by a single vertex, and regarding a dimer incident to this vertex as a bond covering the corresponding lattice edge, the honeycomb lattice \mathcal{L} reduces to a simple quartic

lattice, and dimer coverings on \mathcal{L} lead to vertex configurations of a five-vertex model [4]. Configurations of the five-vertex model are shown in Fig. 2 in the context of a six-vertex model. It is straightforward to verify that we have the correspondence

$$\{\omega_1, \omega_2, \omega_3, \omega_4, \omega_5, \omega_6\} = \{0, w, v, u, \sqrt{\lambda uv}, \sqrt{\lambda uv}\}. \quad (2.2)$$

Here, for definiteness, we assume $\{u, v, w\} > 0$. Note that (2.2) is the most general five-vertex model, since one can always take $\sqrt{\lambda uv} = \sqrt{\omega_5 \omega_6}$, if $\omega_5 \neq \omega_6$.

The partition function of a vertex model is defined as

$$Z = \sum_{\text{config}} \prod_{\text{vertices}} \omega_{k(v)}, \quad (2.3)$$

where the summation is taken over all allowed vertex configurations, the product is over all vertices of the square lattice and $\omega_{k(v)}$ stands for the weight of a vertex v . The case of $\epsilon = 0$ or $\lambda = 1$ leads to the free-fermion model satisfying the free-fermion condition $\omega_1 \omega_2 + \omega_3 \omega_4 = \omega_5 \omega_6$ [8].

For a simple quartic lattice of size $M \times N$, one defines the per-site free energy

$$f(u, v, w; \lambda) \equiv \lim_{M, N \rightarrow \infty} \frac{1}{MN} \ln Z, \quad (2.4)$$

for the five-vertex model. It follows that the per-site generating function for the dimer problem defined in a similar way is $f/2$.

Ordered States: It is instructive to examine the possible ordered states of the dimer lattice. When u , v , or w dominates, the ordered states are those shown respectively in Figs. 3a, 3b, and 3c, where the lattice \mathcal{L} is completely covered by u , v , or w dimers. These are the ordered states occurring in the free-fermion case [4]. But when λ dominates (large positive ϵ), a new ordered state can materialize as shown in Fig. 3d. It is this ordering that adds to new features to the interacting dimer system.

3 The Bethe ansatz equation

To begin with consider the general six-vertex model on a simple quartic lattice of M rows and N columns with periodic boundary conditions in both directions.

Applying transfer matrix in the vertical direction and using the fact that n , the number of empty edges (those not covered by bonds) in a row of vertical edges, is conserved, one can evaluate the partition function (2.3) using the Bethe ansatz [14]. The Bethe ansatz formulation for the general six-vertex model has been given in [9, 15] in a ferroelectric language from which the five-vertex limit does not follow straightforwardly. Here, for completeness, we state the Bethe ansatz equation for the six-vertex model in terms of the vertex weights [16].

In the limit of large M, N , one finds

$$Z \sim \max_{\{n\}} [\Lambda_R(n) + \Lambda_L(n)]^M, \quad (3.1)$$

with

$$\begin{aligned} \Lambda_R(n) &= \omega_1^{N-n} \prod_{j=1}^n \left(\frac{\omega_3\omega_4 - \omega_5\omega_6 - \omega_1\omega_3 z_j}{\omega_4 - \omega_1 z_j} \right) \\ \Lambda_L(n) &= \omega_4^{N-n} \prod_{j=1}^n \left(\frac{\omega_1\omega_2 - \omega_5\omega_6 - \omega_2\omega_4 z_j^{-1}}{\omega_1 - \omega_4 z_j^{-1}} \right), \end{aligned} \quad (3.2)$$

for $n \leq N$, where the n complex numbers z_j , $j = 1, 2, \dots, n$ are the solution of the Bethe ansatz equation

$$z_j^N = (-1)^{n+1} \prod_{i=1}^n \left(\frac{B(z_i, z_j)}{B(z_j, z_i)} \right), \quad j = 1, 2, \dots, n, \quad (3.3)$$

with

$$B(z, z') = \omega_2\omega_4 + \omega_1\omega_3 z z' - (\omega_1\omega_2 + \omega_3\omega_4 - \omega_5\omega_6) z'. \quad (3.4)$$

Note that for fixed $1 \leq n \leq N$, one has generally $\binom{N}{n}$ different $\Lambda_R(n)$ and $\Lambda_L(n)$. It is understood that it is the largest ones for each n that are used in (3.1). We remark that a useful parameter occurring in the analysis of the six-vertex model is

$$\Delta = \frac{\omega_1\omega_2 + \omega_3\omega_4 - \omega_5\omega_6}{2\sqrt{\omega_1\omega_2\omega_3\omega_4}}.$$

It is then clear that $|\Delta| \rightarrow \infty$ in the limit of $\omega_1 \rightarrow 0$, making the five-vertex model a very special limit.

Specializing (3.2) - (3.3) to the five-vertex model weights (2.2), one obtains

$$\begin{aligned} \Lambda_R(n) &= (\beta w)^N \delta_{n,N} \\ \Lambda_L(n) &= u^N \prod_{j=1}^n (x_1 + x_2 z_j), \end{aligned} \quad (3.5)$$

where the z_j 's are to be determined from the Bethe ansatz equation

$$z_j^N = (-1)^{n+1} \prod_{i=1}^n \left(\frac{1 - \beta z_j}{1 - \beta z_i} \right), \quad j = 1, 2, \dots, n \quad (3.6)$$

with

$$x_1 = \frac{w}{u}, \quad x_2 = \frac{v}{u} \lambda, \quad \beta = \frac{v}{w} (1 - \lambda). \quad (3.7)$$

It is clear that Λ_R does not contribute unless $n = N$. But for $n = N$ the partition function can be trivially evaluated. In this case there are no u dimers and hence each row of \mathcal{L} is covered completely by v or w dimers and one has

$$\begin{aligned} Z &= (w^N + v^N)^M, \\ f(u, v, w; \lambda) &= \max\{\ln w, \ln v\}. \end{aligned} \quad (3.8)$$

Alternatively, one can show from (3.5) and (3.6) that $\Lambda_R(N) + \Lambda_L(N) = w^N + v^N$ from which (3.8) also follows. Hence from here on we consider Λ_L only.

Combining (2.4) and (3.1), one has

$$f(u, v, w; \lambda) = \max_{\{n\}} f(n), \quad (3.9)$$

where

$$f(n) = \lim_{N \rightarrow \infty} \frac{1}{N} \ln \Lambda_L(n). \quad (3.10)$$

The prescription of the Bethe ansatz is that, for each fixed n , one solves (3.6) for z_j . This leads to generally many sets of solutions. One next picks the set of solution which gives the largest $f(n)$ for each n . Then, the free energy (3.9) is given by the largest $f(n)$ among all n . We shall refer to the set of z_j which gives rise to the final expression of the partition function (3.9) the maximal set, and the prescription of maximization the maximal principle.

We first point out some immediate consequences of (3.6). First, it is clear that if z_j is solution of (3.6), then its complex conjugate z_j^* is also a solution¹ so that the z_j 's are distributed symmetrically with respect to the real axis. Secondly, for $N = \text{even}$ at least, the negations of β and z_j leave (3.6) unchanged. Thus, if z_j is a solution of (3.6), then $-z_j$ is the solution when β is replaced by $-\beta$.

¹This has the consequence that one must write $z = |z|e^{i\phi}$ with $-\pi \leq \phi \leq \pi$, implying that all branch cuts must be taking along the negative real axis. This observation plays a major role in ensuing considerations.

Combining these two observations, we find the solutions for β and $-\beta$ related by a simple reflection about the imaginary axis. Finally, multiplying the n equations in (3.6), one obtains the identity

$$\left[\prod_{j=1}^n z_j \right]^N = 1. \quad (3.11)$$

4 Noninteracting dimers

It is instructive to apply the Bethe ansatz consideration to the free-fermion case of [4]. In this free-fermion case we have $\{x_1, x_2\} = \{w/u, v/u\}$, $\lambda = 1$, $\beta = 0$, and (3.6) becomes

$$z_j^N = (-1)^{n+1}, \quad j = 1, 2, \dots, n. \quad (4.1)$$

Thus the z_j 's are on the unit circle $|z| = 1$, and can take on any n of the N roots of (4.1). This gives $\binom{N}{n}$ eigenvalues $\Lambda_L(n)$ as expected.

For fixed x_1, x_2 , the maximal set of z_j which gives the largest $\Lambda_L(n)$ for each n is obtained by choosing the n largest $|x_1 + x_2 z_j|$. Now for any n write

$$z_j = e^{i\theta_j}, \quad \alpha = n/N. \quad (4.2)$$

In the limit of large M, N , the z_j 's are distributed continuously on the unit circle with a uniform angular density $N/2\pi$. For fixed α and write $z_\alpha = e^{i\alpha\pi}$, the n largest $|x_1 + x_2 z_j|$ are those given by the z_j 's on the arc of the circle extending from z_α^* to z_α as shown in Fig. 4. One then obtains from (3.5) and (3.10) after replacing n by α in the argument

$$f(\alpha) = \ln u + \frac{1}{2\pi i} \int_{z_\alpha^*}^{z_\alpha} \ln(x_1 + x_2 z) dz. \quad (4.3)$$

The maximal free energy is therefore, after using (3.9),

$$\begin{aligned} f(u, v, w; 1) &= \max_{\{\alpha\}} f(\alpha) \\ &= f(\alpha_0) \\ &= \ln u + \frac{1}{2\pi} \int_{-\alpha_0\pi}^{\alpha_0\pi} \ln(x_1 + x_2 e^{i\theta}) d\theta, \end{aligned} \quad (4.4)$$

where α_0 is determined by

$$f'(\alpha_0) = \ln|x_1 + x_2 z_{\alpha_0}| = 0. \quad (4.5)$$

If $1, x_1, x_2$, or equivalently u, v, w , form a triangle, we have $0 < \alpha_0 < 1$ and $f = f(\alpha_0)$ analytic in u, v, w . If $1, x_1, x_2$, or equivalently u, v, w , do not form a triangle, then there are two possibilities. For $x_1 + x_2 < 1$ or $w + v < u$, we have $|x_1 + x_2 z_j| < 1$ for all z_j , and as a consequence the maximal set is the empty set or, equivalently, $\alpha_0 = 0$. This leads to

$$f(u, v, w; 1) = \ln u. \quad u \geq w + v \quad (4.6)$$

For $|x_1 - x_2| > 1$ or $|w - v| > u$, we have $|x_1 + x_2 z_j| > 1$ for all z_j , so that we take the maximal set $\alpha_0 = 1$ and $z_{\alpha_0} = e^{i\pi}$. This leads to after carrying out the integration in (4.4)

$$\begin{aligned} f(u, v, w; 1) &= \ln u + \max \ln \{x_2, x_1\} \\ &= \max \{\ln v, \ln w\}. \quad u < |w - v| \end{aligned} \quad (4.7)$$

Thus, the phase boundary is

$$|x_1 \pm x_2| = 1, \quad \text{or} \quad |w \pm v| = u. \quad (4.8)$$

These results are in agreement with [4]. The ordered states (4.6) and (4.7) are the frozen states shown in Figs. 3a - 3c in which the dimer lattice \mathcal{L} is completely covered by u, v , or w dimers. The transitions are of second order. We note, in particular, that the phase boundary (4.8) is determined by setting $f'(\alpha_0) = 0$ at $\alpha_0 = 0$, or π , the two points where the path of integration in (4.3) either just emerges or completes a closed contour. The observation of this mechanism underlining the onset of phase transitions proves useful in later considerations.

5 Analysis of the Bethe ansatz equation

We now return to the Bethe ansatz equation (3.6). Define a constant $\overline{\mathcal{C}}(\alpha, \beta)$ by

$$\left[\overline{\mathcal{C}}(\alpha, \beta) \right]^N = (-1)^{n+1} \prod_{j=1}^n (1 - \beta z_j), \quad (5.1)$$

with $\psi_0 \equiv \arg \overline{\mathcal{C}}$ lying in interval $(-\pi/N, \pi/N]$. Then the Bethe ansatz equation (3.6) becomes

$$\left[\overline{\mathcal{C}}(\alpha, \beta) \right]^N z_j^N = (1 - \beta z_j)^{\alpha N}, \quad (5.2)$$

and the N th root of (5.2) gives a trajectory Γ on which all solutions z_j must reside,

$$Ce^{i\psi_0}z_j = (1 - \beta z_j)^\alpha e^{i\phi_j}, \quad \phi_j = 2\pi j/N, \quad j = 1, 2, \dots, N, \quad (5.3)$$

where $C = C(\alpha, \beta) \equiv |\overline{C}(\alpha, \beta)|$. The trajectory Γ is a curve in the complex z plane which is symmetric with respect to the real axis and is given by the equation

$$C|z| = |1 - \beta z|^\alpha. \quad (\Gamma) \quad (5.4)$$

However, by diagonalizing the transfer matrix explicitly for $N \leq 18$, Noh and Kim [17] have found that for $\beta > 1$ the largest eigenvalue assumes the “bounded magnon” ansatz of Noh and Kim [7] in the form of

$$\begin{aligned} z_1 &= \bar{z}_1 \beta^{\alpha N - 1} \\ z_j &= \frac{1}{\beta} \left(1 - \frac{\bar{z}_j}{\beta^{N(1-\alpha)}} \right), \quad j = 2, 3, \dots, n, \end{aligned} \quad (5.5)$$

where $|\bar{z}_j| = 1$ for all j . This says that in the thermodynamic limit of $N \rightarrow \infty$ and $\alpha \neq 0, 1$, one root z_1 resides at infinity while all other roots converge to $1/\beta$. Using this ansatz, one obtains from (5.2)

$$C = 0, \quad \alpha \neq 0, 1, \quad \beta > 1, \quad (5.6)$$

and from (3.5) and (3.10)

$$f(\alpha) = (1 - \alpha) \ln u + \alpha \ln v, \quad \alpha \neq 0, 1, \quad \beta > 1. \quad (5.7)$$

While we shall make use of (5.7) to determine the phase boundary, however, to make our presentation self-contained we shall proceed for the time being without using the ansatz (5.5) and the result (5.7). It will be seen that one is led to the same phase boundary for $\beta > 1$.

Define

$$d \equiv C/|\beta|, \quad d_c \equiv \alpha^\alpha (1 - \alpha)^{1-\alpha}. \quad (5.8)$$

Then, by examining solutions of (5.4) on the real axis, it is straightforward to verify that for $\beta > 0$, Γ assumes the topology shown in Figs. 5a - 5c, respectively for $d > d_c$, $d = d_c$, and $d < d_c$. The topology of Γ for $\beta < 0$ is deduced from those in Fig. 5 by applying a reflection about the imaginary axis, and is shown in Fig. 6. Note that the constant C can be determined once one point on Γ is known.

Particularly, if Γ intersects the negative real axis at $x = -R$, where $R > 0$, then we have

$$C = h(\alpha, R) \equiv \frac{|1 + \beta R|^\alpha}{|R|}. \quad (5.9)$$

Note that, since contours can be deformed as long as they do not cross poles and move along branch cuts, it is the topology of the contours that is important.

In the limit of large N , the distribution of zeroes on Γ becomes continuous. Let $\rho(z)$ be the density of zeroes so that $N \int \rho(z) dz$ over any interval of Γ gives the number of z_j 's in that interval. Then, using (5.3) one finds

$$\rho(z) = \frac{1}{2\pi i} \left(\frac{1}{z} - \frac{\alpha}{z - \beta^{-1}} \right). \quad (5.10)$$

Let Γ_0 be the segment(s) of Γ symmetric with respect to the real axis and on which the maximal set of z_j 's resides. For fixed α , we find as in (4.3) - (4.5),

$$f(\alpha) = \ln u + \frac{1}{2\pi i} \int_{\Gamma_0} \left(\frac{1}{z} - \frac{\alpha}{z - \beta^{-1}} \right) \ln(x_1 + x_2 z) dz, \quad (5.11)$$

$$f(u, v, w; \lambda) = f(\alpha_0), \quad (5.12)$$

where α_0 is the value of α which maximizes $f(\alpha)$.

Note that the α -dependence of the free energy (5.11) for fixed α now enters through both Γ_0 and $\rho(z)$. However they obey two constraints. First, the fact that there are n z_j 's implies

$$\int_{\Gamma_0} \rho(z) dz = \frac{1}{2\pi i} \int_{\Gamma_0} \left(\frac{1}{z} - \frac{\alpha}{z - \beta^{-1}} \right) dz = \alpha. \quad (5.13)$$

In addition, taking the absolute value of (3.11), one obtains

$$\prod_{\Gamma_0} z_j = 1, \quad (5.14)$$

which leads to, in the $N \rightarrow \infty$ limit,

$$\int_{\Gamma_0} \rho(z) \ln z dz = \frac{1}{2\pi i} \int_{\Gamma_0} \left(\frac{1}{z} - \frac{\alpha}{z - \beta^{-1}} \right) \ln z dz = 0. \quad (5.15)$$

For each fixed α , the two constraints (5.13) and (5.15) together with the maximal principle of the free energy are sufficient to determine Γ_0 . Once Γ_0 is known, the

free energy can be evaluated using (5.11) and (5.12). In carrying out integrations along Γ_0 , one is aided by the fact that the path of integration can be deformed as long as it does not cross poles nor run along branch cuts. Care must be taken, however, when Γ_0 intersects branch cuts. When this happens, integration along Γ_0 can be computed by completing the contour into a closed loop and using the Cauchy residue theorem.

In our discussions below we shall also need to evaluate $f'(\alpha)$. Using (5.11) for $f(\alpha)$, generally the α dependence comes in through both the path Γ_0 and the explicit dependence of $\rho(z)$ on α . Let Γ_0 consist of an open path running continuously from z_0^* to z_0 and, in addition to the open path, possibly another closed contour intersecting the real axis. Since Γ_0 can be freely deformed except the terminal points and the intersection points with the branch cut, the derivative of (5.11) with respect to α is derived from three kinds of contributions. First, the two terminal points z_0 and z_0^* will move with α . We write

$$z_0 \equiv R_0 e^{i\theta}, \quad y \equiv \rho(z_0)(dz_0/d\alpha), \quad (5.16)$$

and, due to the fact that the expression (5.10) for $\rho(z)$ contains a factor $1/2\pi i$, we have

$$y^* = -\rho(z_0^*)(dz_0^*/d\alpha). \quad (5.17)$$

Then, the contribution to $f'(\alpha)$ due to the α -dependence of the terminal points gives rise to $y \ln(x_1 + x_2 z_0) + y^* \ln(x_1 + x_2 z_0^*)$. Secondly, if Γ_0 consists of another closed contour intersecting the branch cut in (5.11) at one or two points $z_r < 0$, then since the integration path can be deformed, the α -dependence is through the intercepts z_r only (which now moves along the branch cut), the contribution due to z_r can be treated as in the above. Namely, we regard two points just above and below z_r as two terminal points. This leads to a contribution of $2\pi i \sum_r y_r$, where

$$y_r = \rho(z_r)(dz_r/d\alpha) = \text{pure imaginary} = -y_r^*, \quad (5.18)$$

and this contribution is the same for all branch cuts. Thirdly, there is a contribution due to the second term in $\rho(z)$ as shown in (5.10). Combining the three, one obtains

$$\begin{aligned} f'(\alpha) = & y \ln(x_1 + x_2 z_0) + y^* \ln(x_1 + x_2 z_0^*) \\ & + 2\pi i \sum_r (\pm y_r) - \frac{1}{2\pi i} \int_{\Gamma_0} \frac{\ln(x_1 + x_2 z)}{z - \beta^{-1}} dz, \end{aligned} \quad (5.19)$$

where the \pm sign is determined by the orientation of Γ_0 at the intercepts.

Finally, it is clear from (5.11) and (5.19) that, in carrying out the contour integrations for $f(\alpha)$ and $f'(\alpha)$, it is important to determine the location of the branch point $-x_1/x_2$ relative to the contour Γ_0 . First, from the readily verified identity

$$(1 - \beta) - \frac{x_2}{x_1} = 1 - \frac{v}{w}, \quad (5.20)$$

one locates the branch point $-x_1/x_2$ by

$$\begin{aligned} x_1/x_2 &> (1 - \beta)^{-1}, & w > v \\ &< (1 - \beta)^{-1}, & w < v, \end{aligned} \quad (5.21)$$

We remark that from the inequality

$$x_1/x_2 < |\beta|^{-1}, \quad \beta < 0. \quad (5.22)$$

one has (see below) for Fig. 6c the inequality $R > R_1 > |\beta|^{-1} > x_1/x_2$, implying that the points $x = -R, -R_1$ are both on the branch cut. We further relate $\sum_r y_r$, y , and y^* by taking the derivatives of (5.13) and (5.15) with respect to α , obtaining

$$y + y^* = 1 + \frac{1}{2\pi i} \int_{\Gamma_0} \frac{dz}{z - \beta^{-1}} \quad (5.23)$$

$$y \ln z_0 + y^* \ln z_0^* + 2\pi i \sum_r (\pm y_r) = \frac{1}{2\pi i} \int_{\Gamma_0} \frac{\ln z}{z - \beta^{-1}} dz. \quad (5.24)$$

It now follows from (5.19) - (5.24) that we have

$$f'(\alpha) = y \ln \left(\frac{x_1}{z_0} + x_2 \right) + y^* \ln \left(\frac{x_1}{z_0^*} + x_2 \right) + \frac{1}{2\pi i} \int_{\Gamma_0} \frac{\ln z - \ln(x_1 + x_2 z)}{z - \beta^{-1}} dz, \quad (5.25)$$

provided that y_r 's in (5.19) and (5.24) are the same, namely, Γ_0 cuts both branch cuts at the same points. In section 7 we shall compute $f'(\alpha)$ using (5.25) which applies to all cases and all α , including the case that Γ_0 consists of an open path as well as a closed contour. The derivative $f'(\alpha)$ near the phase boundaries will also be computed in section 8 by analyzing small perturbations of the free energy.

6 The contour Γ at $\alpha = 0, 1-, 1$, and $1/2$

In our discussions we shall need to evaluate integrals at $\alpha_0 = 0, 1-, 1$, and $1/2$. It turns out that the contours Γ for $\alpha = 1$ and $\alpha = 1-$ should be considered with care. In this section we consider the contour Γ at these special points.

(a) $\alpha = 0$. This is the case that Γ_0 begins to emerge with very few z_j 's. The constraint (5.14) then dictates that $z_0 \sim 1$ and, using (5.4) and (5.14), one finds $\overline{C}(0, \beta) = 1$ and Γ the unit circle.

(b) $\alpha = 1$. This is the case of $n = N$ when one picks all N z_j 's and hence $\Gamma_0 = \Gamma$. One can use (5.2) to obtain

$$\left[\overline{C}^N(1, \beta) - (-\beta)^N \right] z_j^N + \cdots - 1 = 0. \quad (6.1)$$

Using (6.1), the constraint (5.14) leads to the relation

$$C^N(1, \beta) = \left| 1 - \beta^N \right|, \quad (6.2)$$

or, in the thermodynamic limit,

$$\begin{aligned} C(1, \beta) &= 1, & |\beta| < 1 \\ &= |\beta|, & |\beta| > 1 \end{aligned} \quad (6.3)$$

One also finds from (5.8) that $d_c = 1$ for $\alpha = 1$, and hence

$$d > d_c, \quad |\beta| < 1 \quad (6.4)$$

$$= d_c, \quad |\beta| > 1. \quad (6.5)$$

The trajectory Γ_0 is, from (5.4) with $C = C(1, \beta)$,

$$\left| \frac{1}{z} - \beta \right| = 1, \quad |\beta| < 1 \quad (6.6)$$

$$\left| \frac{1}{\beta z} - 1 \right| = 1, \quad |\beta| > 1. \quad (6.7)$$

The contour (6.6) for $|\beta| < 1$ is a circle of radius $(1 - \beta^2)^{-1}$ centered at $x = -\beta/(1 - \beta^2)$ on the real axis, where $x = \text{Re}(z)$. Particularly, the circle intersects the real axis at $x = -R_2, R_1$, where

$$R_2 = (1 - \beta)^{-1}, \quad R_1 = (1 + \beta)^{-1}, \quad (6.8)$$

The contour (6.7) for $|\beta| > 1$ is the vertical straight line $x = (2\beta)^{-1}$.

It is readily verified that by integrating along the contours (6.6) and (6.7), one has

$$\frac{1}{2\pi i} \int_{\Gamma} \rho(z) \ln z dz = 0, \quad |\beta| < 1 \quad (6.9)$$

$$= -\ln |\beta| \quad |\beta| > 1. \quad (6.10)$$

Thus, the constraint (5.13) is not satisfied for $|\beta| > 1$, indicating that the $\alpha = 1$ solution is spurious.² This leads us to consider instead the $\alpha = 1-$ solution as a limit to $\alpha = 1$.

(c) $\alpha = 1-$.

We consider the cases $\beta > 0$ and $\beta < 0$ separately.

For $\beta > 0$, the contours are those shown in Fig. 5. In all cases, since the branch cuts are on the negative axis, the contour can be deformed to form a single closed contour intersecting the real axis at two points and enclosing the origin. Let the intersecting point on the negative real axis be $x = -R$. One finds from (5.15) the relation

$$\ln h(\alpha, R) = 0, \quad (6.11)$$

where $\alpha = 1-$, $h(\alpha, R)$ is defined in (5.9) and is equal to C . Thus, one obtains $C = 1$. In addition, one can solve for R from (6.11) and obtains

$$\begin{aligned} R &= (1 - \beta)^{-1}, & \beta < 1 \\ R &= |\beta|^{\alpha/(1-\alpha)} \rightarrow \infty, & \beta > 1. \end{aligned} \quad (6.12)$$

Thus, the intercept with the negative axis R for $\beta < 1$ is the same as that given in (6.8). Once $C = 1$ is known, one can compute the location of other intercept(s) with the real axis which will be all positive including the intercept $(1 + \beta)^{-1}$ given by (6.8). Note that the second line of (6.12) (and what follows) is what one would obtain without making use of the bounded magnon ansatz (5.5). In this case the precise location of the other two intercepts (for $\beta > 1$, see below) does not concern us since the contour can be deformed freely in the $x > 0$ plane as long as it does not cross the pole at β^{-1} .

For $\beta < 0$ the contours are those shown in Fig. 6. Consider first Fig. 6a where the contour intersects the negative real axis at one point at $x = -R$, one

²However, if one carries out the product $\prod_{\Gamma_0} z_j$ in the RHS of (5.14) for finite N , one can show that (5.14) is satisfied.

finds again $C = 1$ and the two intercepts (6.8) with $R = (1 - \beta)^{-1}$. In the case of Fig. 6c where Γ intersects the real axis at four points as shown with $-R < -R_1 < -R_2 < R_3$, generally the contour cannot be deformed into a single loop due to the presence of the branch cuts. But the integration (5.15) can be carried out as in the above yielding

$$-\ln h(\alpha, R_1) + \ln h(\alpha, R_2) + \ln h(\alpha, R) = 0, \quad (6.13)$$

where

$$h(\alpha, R) = h(\alpha, R_1) = h(\alpha, R_2) = h(\alpha, -R_3) = C. \quad (6.14)$$

The identities (6.13) and (6.14) can hold only for $C = 1$,

$$R_1 = (|\beta| - 1)^{-1}, \quad R_2 = (|\beta| + 1)^{-1}, \quad (6.15)$$

which is the same as (6.8), and both R and R_3 diverging as in the second line of (6.12). Note in particular that R_2 coincides with $R = (1 - \beta)^{-1}$ in (6.8) of Fig. 5a. Now we have again from (5.8) $d_c = 1$ for $\alpha = 1-$. Thus, in contradistinction to (6.3), one finds $C(1-, \beta) = 1$ for all β and therefore

$$d = \frac{1}{|\beta|} > d_c, \quad |\beta| < 1 \quad (6.16)$$

$$< d_c, \quad |\beta| > 1. \quad (6.17)$$

Thus, the contour Γ consists of two loops when $|\beta| > 1$, with the outer loop residing in the infinite regime.

We note that while (6.16) is the same as (6.4), (6.17) is different from (6.5). Finally, one verifies that, by deforming Γ into a closed contour enclosing the origin but not β^{-1} , the constraint (5.13) is identically satisfied for all β .

(d) $\alpha = 1/2$.

We are primarily interested in the free energy and its derivatives near a phase transition point which, as in the nonintersecting case, occurs when the maximal contour either closes or just begin to emerge. Thus, for $\alpha = 1/2$, we consider the cases shown in Figs. 5c and 6c when the contour Γ consists of two loops and Γ_0 is one of the two loops. But this cannot happen for $\beta > 0$. When $\beta > 0$ the inner loop and portion of the outer loop are in the $x > 0$ half plane. Then Γ_0 in the maximal solution of the free energy (5.11) cannot be either of the two loops, since some points on the other loop will have larger values of $\ln(x_1 + x_2 z)$. Hence

$\alpha = 1/2$ can occur only for $\beta < 0$. This conclusion is also expected on physical grounds, that the $\alpha = 1/2$ ordered state in Fig. 3d dominates only when the interaction between neighboring u and v dimers is sufficiently attractive, namely, when λ is sufficiently large or β sufficiently negative.

For $\beta < 0$ the contour Γ intersects the negative real axis (and the branch cut of $\ln z$) at three points. One verifies after some algebra the identity

$$\int_{\text{inner loop}} \rho(z) dz = \alpha \ln|z_0| \neq \alpha,$$

for any α . Therefore Γ_0 must be the outer loop.

Taking the outer loop as Γ_0 , we have firstly from the constraint (5.13)

$$\alpha = \frac{1}{2\pi i} \int_{\Gamma_0} \left(\frac{1}{z} - \frac{\alpha}{z - \beta^{-1}} \right) dz = 1 - \alpha,$$

leading to the correct value $\alpha = 1/2$. The constraint (5.15) now yields

$$\begin{aligned} 0 &= \frac{1}{2\pi i} \int_{\Gamma_0} \left(\frac{1}{z} - \frac{1/2}{z - \beta^{-1}} \right) \ln z dz \\ &= \ln R - \frac{1}{2} \ln(R + \beta^{-1}), \end{aligned} \tag{6.18}$$

or, equivalently,

$$R^2 - R - \beta^{-1} = 0. \tag{6.19}$$

This yields the solutions

$$R_{\pm} = \frac{1}{2} \left(1 \pm \sqrt{1 - \frac{4}{|\beta|}} \right). \tag{6.20}$$

Thus, we see that, as expected, (6.20) has solution only for sufficiently negative $\beta < -4$.

Furthermore, when Γ_0 is a closed contour, one has from (5.9), (5.8) and using (6.20),

$$C\left(\frac{1}{2}, \beta\right) = \sqrt{|\beta|}, \quad d_c = \frac{1}{2}, \tag{6.21}$$

and

$$d = \frac{1}{\sqrt{|\beta|}} < d_c, \quad \beta < -4. \tag{6.22}$$

Thus, Γ consists of two loops only when $\beta < -4$. In this case Γ intercepts the real axis at the four points $-R < -R_1 < -R_2 < R_3$ as shown in Fig. 6c and determined from $C|x| = \sqrt{|1 - \beta x|}$. This leads to

$$\begin{aligned} R &= R_+, & R_1 &= R_- \\ R_2 &= \frac{1}{2} \left(\sqrt{1 + \frac{4}{|\beta|}} - 1 \right), & R_3 &= \frac{1}{2} \left(\sqrt{1 + \frac{4}{|\beta|}} + 1 \right). \end{aligned} \quad (6.23)$$

In summary, we have found that, for $\alpha = 1-$, we have $C = 1$ and Γ consists of one loop for $|\beta| < 1$ which intersects the real axis at (6.8), and two loops for $|\beta| > 1$ intersecting the real axis at 4 points. In the latter case when $\beta > 1$, the contour can be deformed into one loop enclosing the origin and therefore the situation is the same as for $|\beta| < 1$. In the case of $\beta < -1$ the outer loop resides in the infinite regime. For $\beta < 1$, the intercept of Γ on the negative axis and closest to the origin is at $x = -(1 - \beta)^{-1}$. For $\alpha = 1/2$, one finds $C = \sqrt{|\beta|}$ and that, for $\beta < -4$, Γ consists of two loops intersecting the real axis at the four points given by (6.23).

7 The phase diagram

Ideally one would like to proceed at this point to compute the free energy (5.12) from which the complete thermodynamics of the dimer system can be determined. However, as this evaluation involves path integrations which generally cannot be put into closed forms, we shall in the next section apply small perturbations to the free energy near the phase boundaries. We proceed here to first determine the phase boundaries and the phase diagram.

Guided by the analysis of the $\lambda = 1$ solution of section 4, we expect singularities of the free energy (5.12) to occur when either the maximal path Γ_0 contains a small emerging segment or when it completes a closed contour. As in the case of $\lambda = 1$, this will happen at $\alpha_0 = 0$ (segment emerging) and $\alpha_0 = 1$ (closed contour) leading to the ordered states shown in Figs. 3a - 3c. In addition, we expect another singularity of the free energy to occur at $\alpha_0 = 1/2$ for $\beta < -4$ as Γ_0 completes the outer loop of two closed contours, leading to the order state shown in Fig. 3d. In all these cases the free energy $f(\alpha)$ should be the maximal solution at $\alpha = \alpha_0 = 0, 1$, or $1/2$, and the phase boundary is given by $f'(\alpha_0) = 0$

provided that $f(\alpha)$ is concave at α_0 . Once the contours Γ_0 is known, both the free energy (5.11) and its derivative (5.25) can be evaluated at $\alpha = 0, 1, 1/2$.

Consider first $\alpha = 0$. This is the case that Γ_0 begins to emerge at $z_0 = R_0 e^{i\theta} \sim 1$ and $y + y^* = 1$. It then follows from (5.11) and (5.25) that we have, for $\beta < 1$ at least,

$$\begin{aligned} f(0) &= \ln u, \\ f'(0) &= \ln\left(\frac{w + \lambda v}{u}\right). \end{aligned} \quad (7.1)$$

For $\alpha = 1$, (or more precisely $\alpha = 1 -$) and $1/2$, both integrals (5.11) and (5.25) can be evaluated using the contours Γ_0 determined in the preceding section. We leave details of the evaluations elsewhere, and collect here the results.

For $\alpha = 1$ one finds, for $\beta > 1$,

$$\begin{aligned} f(1) &= \ln v, \\ f'(1) &= \ln(v/u), \end{aligned} \quad (7.2)$$

and, for $\beta < 1$,

$$\begin{aligned} f(1) &= \max\{\ln w, \ln v\} \\ f'(1) &= \ln\left(\frac{w(w-v)}{wu - uv(1-\lambda)}\right), & w > v \\ &= \ln\left(\frac{v-w}{\lambda u}\right). & v > w \end{aligned} \quad (7.3)$$

For $\alpha = 1/2$ one finds, for $\beta < -4$,

$$\begin{aligned} f\left(\frac{1}{2}\pm\right) &= \frac{1}{2} \ln(\lambda uv) \\ f'\left(\frac{1}{2}\pm\right) &= \ln\left[\frac{v\lambda}{u}\left(1 - \frac{w}{v\lambda R_{\mp}}\right)^2\right], \end{aligned} \quad (7.4)$$

where R_{\pm} is given by (6.20).

To ensure that the free energy $f(\alpha_0)$ is indeed the maximal solution and that $f'(\alpha_0) = 0$ is a phase boundary, we need to ascertain that $f(\alpha_0)$ is a maximum. This turns out to be a delicate matter for $\alpha_0 = 0, 1$, as detailed calculations show that $f''(\alpha_0) = 0$. However, one can proceed as follows.

First consider the case $\beta > 1$. As discussed in Sec. 5 and guided by numerical evidence, the ground state is given by the bounded magnon solutions (5.5) with the free energy $f(\alpha)$ given by (5.7). It follows that the maximal free energy is

$$f(u, v, w; \lambda) = \max \{\ln u, \ln v\}, \quad w < v(1 - \lambda). \quad (7.5)$$

and the phase boundary for $\beta > 1$ is $f(0+) = f(1-)$, or

$$u = v \quad \text{for } w < v(1 - \lambda). \quad (7.6)$$

Alternately, one can also arrive at the same phase boundary (7.6) without invoking (5.5) and (5.7): Assuming that $f(\alpha)$ is either concave or convex in $0 \leq \alpha \leq 1$, it is easy to see that $f'(0) = 0$ and $f'(1) = 0$ cannot be the phase boundary for $\beta > 1$. This follows from the observations that, using (7.1),

$$\begin{aligned} f'(0) \geq 0 &\rightarrow w + \lambda v \geq u \\ &\rightarrow v > u \quad (\text{using } \beta > 1 \text{ or } w + \lambda v < v) \\ &\rightarrow f'(1) > 0, \end{aligned} \quad (7.7)$$

and using (7.2),

$$\begin{aligned} f'(1) \leq 0 &\rightarrow v \leq u \\ &\rightarrow u > w + \lambda v \quad (\text{again using } \beta > 1) \\ &\rightarrow f'(0) < 0. \end{aligned} \quad (7.8)$$

Thus, for $\beta > 1$, in the former case, $f'(0) = 0$ is not a phase boundary since $f(0) < f(1)$, and in the latter case $f'(1) = 0$ is not a phase boundary since $f(1) < f(0)$. Furthermore, relations (7.7) and (7.8) are consistent with the fact that the maximal free energy occurs at, respectively, the frozen states $\alpha_0 = 1$ and $\alpha_0 = 0$. It follows that the accompanying transition is between the two frozen phases and is thus of first order.

However, the phase boundary are given correctly by $f'(0) = 0$ and $f'(1) = 0$ for $\beta < 1$. This can be seen as follows.

For $f(0)$ to be a maximum we have always $f'(0) \leq 0$, and for $f(1)$ a maximum we have $f'(1) \geq 0$. We find that, for $\beta < 1$ or $(1 - \lambda)v < w$, one has

$$f'(0) \leq 0 \rightarrow f'(1) < 0 \quad (7.9)$$

$$f'(1) \geq 0 \rightarrow f'(0) > 0. \quad (7.10)$$

Thus, under the same convexity and concavity assumption, $f(0)$ and $f(1)$ can indeed be the maximum of the free energy. Thus, the phase boundaries are $f'(0) = 0$ and $f'(1) = 0$ and the accompanying transition is continuous. Explicitly, the phase boundaries are, at $\alpha_0 = 0$,

$$w + \lambda v = u \quad \text{for } (1 - \lambda)v < w \quad (7.11)$$

and, at $\alpha_0 = 1$,

$$\lambda = \left(\frac{w}{u} - 1\right)\left(\frac{w}{v} - 1\right) \quad \text{for } w > v \quad (7.12)$$

$$v = w + \lambda u \quad \text{for } w + \lambda v > v > w. \quad (7.13)$$

Finally, for the phase boundary at $\alpha_0 = 1/2$, we observe from (7.4) that, for $\beta < -4$, $f'(\alpha)$ is discontinuous at $\alpha = 1/2$ with

$$f\left(\frac{1}{2}-\right) > f\left(\frac{1}{2}+\right). \quad (7.14)$$

Then $f(\alpha)$ is a maximum at $\alpha = 1/2$ provided that we have

$$f\left(\frac{1}{2}-\right) \geq 0 \quad \text{and} \quad f\left(\frac{1}{2}+\right) \leq 0. \quad (7.15)$$

The phase boundary is therefore the borderline cases $f(\frac{1}{2}-) = 0$ and $f(\frac{1}{2}+) = 0$ when $f(\frac{1}{2})$ begins to exhibit a maximum. Now, for $\beta < -4$ and writing $v\lambda - |\beta|w = v$, it can be readily verified that we have

$$v\lambda - \frac{w}{R_{\pm}} \geq v > 0. \quad (7.16)$$

Thus, the phase boundary at $\alpha_0 = 1/2$ is, from (7.4),

$$v\lambda - \frac{w}{R_{\pm}} = \sqrt{\lambda uv}. \quad (7.17)$$

Explicitly, (7.17) can be written as

$$uv\lambda^3 - [w^2 + 2w(u + v) + u^2 + v^2]\lambda^2 + [2w^2 + 2w(u + v) + uv]\lambda - w^2 = 0, \quad (7.18)$$

which reflects its full symmetry with respect to u and v .

The phase diagram. Since the vertex weights (2.2) are arbitrary to an overall constant and since there exists an expected u, v symmetry, it is convenient to consider the phase diagram in the parameter space $u/w, v/w, \lambda$. We have found the existence of five regimes W ($\alpha_0 = 0$), U ($\alpha_0 = 1$), V ($\alpha_0 = 1$), Λ ($\alpha_0 = 1/2$) and D (disordered). The regimes U, V, W, Λ are phases in which dimers are frozen in respective configurations of Figs. 3a,b,c,d with values of α_0 fixed as indicated. The phase boundaries are given by (7.6), (7.11), (7.12), (7.13), and (7.6), leading to the phase diagrams shown in Fig. 9.

For $\lambda = 1$, the noninteracting case, the phase diagram is shown in Fig. 9a, and the boundaries separating regimes W/D , U/D , and V/D are given respectively by (7.11), (7.13), (7.12).

For $\lambda > 1$ corresponding to attractive interactions between u and v dimers, a new ordered phase Λ with $\alpha_0 = 1/2$ arises. A typical phase diagram is shown in Fig. 9b, where, in addition to those phase boundaries already present in Fig. 9a, a new phase boundary (7.18) separates regimes D and Λ .

For $\lambda < 1$ corresponding to repulsive interactions between u, v dimers, a typical phase diagram is shown in Fig. 9c. In addition to the boundaries already present in Fig. 9a, regimes U and V now share a boundary given by (7.6), namely $u = v > w/(1 - \lambda)$, across which there is a first-order transition. This leads to the existence of a special transition point at $u = v = w/(1 - \lambda)$. It is a point where two lines of continuous transition merge into a first order line and maybe called a kind of tricritical point. However, it is different from ordinary tricritical points in that the discontinuity along the first order line does not vanish at that point.

8 The critical behavior and expansions of the free energy near phase boundaries

In this section we derive expansions of the free energy (5.11) for small deviations near phase boundaries, and use the expansions to obtain the critical behavior in the disorder regime.

The phase boundaries are characterized by $\alpha \sim 0, 1$ and $1/2$ and, in all cases Γ_0 can be deformed into a single trajectory extending from a point z_0^* to its complex conjugation z_0 . Thus, we write

$$z_0 = R_0 e^{i\theta}, \quad z_0 - \beta^{-1} = A e^{i\phi} \quad (8.1)$$

where $R_0 > 0, A > 0, 0 < \{\theta, \phi\} < \pi$. We consider $\theta, \phi \sim 0$ or π , and there are three cases to consider.

(a) $\alpha = 0$: In this case Γ_0 is a small arc of radius R_0 extending from angle $-\theta$ to θ .

For $0 < \beta R_0 < 1$, for example, (5.13) can be written as

$$\alpha = \frac{\theta}{\pi} - \alpha \frac{\phi - \pi}{\pi}. \quad (8.2)$$

Similarly, for the cases $\beta R_0 > 1$ and $\beta < 0$, we obtain

$$\alpha = \frac{\theta}{\pi} - \alpha \frac{\phi}{\pi}. \quad (8.3)$$

Furthermore, in all cases R_0 , A and $|\beta|^{-1}$ form a triangle implying the relation

$$R_0 : A : |\beta|^{-1} = \sin \phi : \sin \theta : |\sin(\phi - \theta)|. \quad (8.4)$$

Thus, one obtains

$$R_0 = \frac{\sin \phi}{\beta \sin(\phi - \theta)}, \quad A = \frac{\sin \theta}{\beta \sin(\phi - \theta)}, \quad (8.5)$$

where β always has the same sign as $\phi - \theta$. For given α and β , either (8.2) or (8.3) and the expression of R_0 in (8.5) relates R_0 to θ . To determine R_0 and θ individually, another relation connecting R_0 and θ is needed. This is provided by (5.15).

For all cases, (5.15) can be written as

$$0 = \ln R_0 + \frac{1}{2\pi} \int_0^\theta \ln \left| \frac{R_0 e^{i\varphi} - \beta^{-1}}{R_0 e^{i\theta} - \beta^{-1}} \right|^2 d\varphi. \quad (8.6)$$

Thus, R_0 and θ can be generally determined, although implicitly.

Now we specialize the above consideration to small α . When α is small, θ is also small. Then, expanding (8.1) and (8.6), one obtains $R_0 = 1 + O(\theta^3)$, $A = |1 - \beta^{-1}| + O(\theta^2)$ and

$$\theta \left[1 + \frac{\alpha}{(\beta R_0)^{-1} - 1} \right] = \alpha \pi, \quad (8.7)$$

establishing that $\theta \sim \alpha\pi$.

Using (8.2), (8.3) and the small angle expansion (8.7), one finds after some algebra that in all cases the expansion of the free energy (5.11) at $\alpha = 0$ is

$$f(\alpha) = \ln u + \alpha \ln(x_1 + x_2) - \frac{\alpha^3 \pi^2}{6} \left(\frac{x_1 x_2}{(x_1 + x_2)^2} \right) + O(\alpha^4). \quad (8.8)$$

Note that the corresponding expression Eq. (34) of [7] contains a typographical error.

(b) $\alpha = 1$: In this case the contour Γ_0 is almost a closed loop, and can be considered as a closed loop Γ' intercepting the negative real axis at $-R_0$ plus a small arc extending from z_0^* to z_0 . Now we have always $\theta \sim \pi$ and, depending on whether $\phi \sim \pi$ ($\beta > 0$) or $\phi \sim 0$ ($\beta < 0$), we have the two cases to consider. Thus, (5.13) leads to

$$\begin{aligned} \alpha &= 1 + \frac{\theta - \pi}{\pi} - \alpha \frac{\phi - \pi}{\pi}, & \beta > 0 \\ &= 1 + \frac{\theta - \pi}{\pi} - \alpha \frac{\phi}{\pi}, & \beta < 0 \end{aligned} \quad (8.9)$$

We again find (8.5) hold for all β , and that, (5.15) leads to

$$0 = \alpha \left[\ln R_0 - \ln |\beta A| - \frac{1}{2\pi} \int_0^{\pi-\theta} \ln \left| \frac{R_0 e^{i\varphi} + \beta^{-1}}{R_0 e^{i(\pi-\theta)} + \beta^{-1}} \right|^2 d\varphi \right]. \quad (8.10)$$

We now specialize to $\alpha = 1 -$ and $\theta = \pi -$. Expanding (8.10) and (8.9), one obtains $R_0 = (1 - \beta)^{-1} + O[(\pi - \theta)^2]$, $A = |(1 - \beta)^{-1} + \beta^{-1}| + O[(\pi - \theta)^2]$ and

$$(\pi - \theta) \left[1 - \frac{\alpha}{(\beta R_0)^{-1} + 1} \right] = (1 - \alpha)\pi. \quad (8.11)$$

It then follows that, after using (5.20), (8.9), (8.11) and some lengthy algebra, one arrives at the expansion valid for all β ,

$$\begin{aligned} f(\alpha) &= \ln v + (\alpha - 1) \left[\ln \left(x_2 - x_1(1 - \beta) \right) + \ln \left(\frac{x_1}{x_2} \beta + 1 \right) \right] \\ &\quad + \frac{(\alpha - 1)^3 \pi^2}{6} \left(\frac{x_2 [x_1 - \beta(x_1 \beta + x_2)]}{(1 - \beta)^2 [x_2 - (1 - \beta)x_1]^2} \right), \\ &\quad \text{for } R_0 \sim (1 - \beta)^{-1} > x_1/x_2, \\ &= \ln w + (\alpha - 1) \ln \left[x_1 - \frac{x_2}{1 - \beta} \right] + \frac{(\alpha - 1)^3 \pi^2}{6} \left[\frac{x_1(x_1 \beta + x_2)}{[x_2 - (1 - \beta)x_1]^2} \right], \\ &\quad \text{for } R_0 \sim (1 - \beta)^{-1} < x_1/x_2. \end{aligned} \quad (8.12)$$

(c) $\alpha = 1/2$: In this case the contour Γ_0 (after some deformation in the case of $\alpha = \frac{1}{2}+$) is a closed loop plus a small arc running from z_0^* to z_0 , both intercepting the negative axis at $-R_0$ for $\alpha \sim \frac{1}{2} \pm$. Since $-R_{\pm} < \beta < 0$, we have always $\theta, \phi \sim \pi$. Therefore (5.13) yields

$$\alpha = 1 - \alpha + \frac{\theta - \pi}{\pi} - \alpha \frac{\phi - \pi}{\pi}. \quad (8.13)$$

One also finds R_0, A given by (8.5). In addition, (5.15) now leads to

$$0 = 2 \ln R_0 - \ln A - \frac{1}{2\pi} \int_0^{\pi-\theta} \ln \left| \frac{R_0 e^{i\varphi} + \beta^{-1}}{R_0 e^{i(\pi-\theta)} + \beta^{-1}} \right|^2 d\varphi. \quad (8.14)$$

Thus, one obtains $R_0 = R_{\mp} + O[(\pi - \theta)^2]$, $A = R_{\mp} + \beta^{-1} + O[(\pi - \theta)^2]$,

$$(\pi - \theta) \left[1 - \frac{\alpha}{(\beta R_0)^{-1} + 1} \right] = 2 \left(\frac{1}{2} - \alpha \right) \pi, \quad (8.15)$$

from which one deduces after some lengthy algebra the expansion

$$\begin{aligned} f(\alpha) = & \frac{1}{2} \ln(\lambda uv) + \left(\alpha - \frac{1}{2} \right) \ln \left(\frac{(x_1 - x_2 R_{\mp})^2}{x_2 R_{\mp}^2} \right) \\ & + \left(\frac{2(\alpha - 1/2)^3 \pi^2}{3(R_{\mp} - 1/2)^3} \right) D(x_1, x_2, \beta), \end{aligned} \quad (8.16)$$

where

$$D(x_1, x_2, \beta) = \beta^{-1} + \frac{2x_1 x_2 R_{\mp}^4}{(x_1 - x_2 R_{\mp})^2} - \frac{(x_1 + x_2 \beta^{-1}) x_2 R_{\mp}^2}{(x_1 - x_2 R_{\mp})^2}. \quad (8.17)$$

Here, the upper (lower) sign pertains to $\alpha > 1/2$ ($\alpha < 1/2$). This is an extension of the corresponding expressions Eqs. (58), (68) and (69) of [7].

The critical behavior. We have obtained expansions of the free energy (5.11) in the disorder regime near the phase boundaries $\alpha_0 = 0, 1, 1/2$ to be given by, respectively, (8.8), (8.12), and (8.16). It is now a simple matter to verify that, in all cases, the maximal free energy assumes the form

$$f[\alpha_0(t)] = f[\alpha_0(0)] + c(u, v, w, \lambda) t^{3/2}, \quad (8.18)$$

where t is some measure of a small deviation from the phase boundary in the parameter space, $c(u, v, w, \lambda)$ is a function regular in t , and $\alpha_0(t)$ is the value of

α determined from the maximal principle. Considered as a vertex model [4], for example, t can be $|T - T_c|$, where T_c is the critical temperature. It then follows from (8.18) that the transition is of second order (continuous) and the specific exponent is $\alpha = 1/2$. This is exactly the same critical behavior of noninteracting dimers [3, 5], and is also the critical behavior expected from the Pokrovsky–Talapov type transitions [6]. In order to check the internal consistency of our results, however, we shall define $t > 0$ by writing in respective equations for the phase boundary $w \rightarrow w(1+t)$, or $w \rightarrow w(1-t)$ to ensure in the disorder regime. We then expect the resulting expression for $c(u, v, w, \lambda)$ to reflect a $\{u, v\}$ and $\alpha_0 = \{0, 1\}$ symmetry.

To verify (8.18), we apply the maximal principle to the free energy (8.8), (8.12), and (8.16). Consider first (8.8), the expansion of $f(\alpha)$ at $\alpha = 0$, for which the phase boundary is $x_1 + x_2 = 1$ or $u = w + \lambda v$. Near the phase boundary we write $w = w(1+t)$, where t is small, and determine $\alpha_0(t)$ from

$$f'[\alpha_0(t)] = \ln\left(1 + \frac{w}{u}t\right) - \frac{[\alpha_0(t)]^2\pi^2}{2}\left(\frac{x_1x_2}{(x_1+x_2)^2}\right) = 0. \quad (8.19)$$

Substituting this $\alpha_0(t)$ into (8.8) and expanding for small t , one obtains

$$f[\alpha_0(t)] = \ln u + \frac{2w}{3\pi}\sqrt{\frac{2}{uv\lambda}}t^{3/2}. \quad (8.20)$$

This leads to (8.18).

Consider next (8.12), the expansion of $f(\alpha)$ at $\alpha = 1$. For the first line of (8.12), the phase boundary is (7.13) or $v = w + \lambda u$. Near the phase boundary we define t by writing $w \rightarrow w(1+t)$ in (7.13) and obtain

$$\begin{aligned} f'[\alpha_0(t)] &= \ln\left(1 - \frac{w}{\lambda u}t\right) + \frac{[\alpha_0(t) - 1]^2\pi^2}{2}\left(\frac{x_2[x_1 - \beta(x_1\beta + x_2)]}{(1-\beta)^2[x_2 - (1-\beta)x_1]^2}\right) \\ &= 0. \end{aligned} \quad (8.21)$$

This leads to

$$f[\alpha_0(t)] = \ln v + \frac{2w}{3\pi}\sqrt{\frac{2}{uv\lambda}}t^{3/2}. \quad (8.22)$$

Note that (8.20) and (8.22) reflect the expected $\{u, v\}$ and α_0 symmetry.

For the second line of (8.12), the phase boundary is $x_1 - x_2/(1 - \beta) = 1$ or (7.12). Near the phase boundary we define t by writing $w \rightarrow w(1 - t)$ in (7.12) and obtain

$$\begin{aligned} f'[\alpha_0(t)] &= \ln\left(1 - \frac{2w - u - v}{w - v}t\right) + \frac{[\alpha_0(t) - 1]^2\pi^2}{2} \left(\frac{x_1(x_1\beta + x_2)}{[x_2 - (1 - \beta)x_1]^2}\right) \\ &= 0. \end{aligned} \quad (8.23)$$

This leads to

$$f[\alpha_0(t)] = \ln w - t + \frac{2}{3\pi} \sqrt{\frac{2(2w - u - v)^3}{\lambda uv(u + v)}} t^{3/2}. \quad (8.24)$$

Here the term linear in t comes from the first term in (8.24) and does not contribute to the “specific heat” exponent.

Finally, Consider (8.16), the expansion of the free energy at $\alpha = 1/2$. Near the phase boundary $v\lambda - w/R_{\pm} = \sqrt{\lambda uv}$ or (7.18), we define t by writing $w = w(1 - t)$ in (7.18). Then $\alpha_0(t)$ is determined from

$$\begin{aligned} f'[\alpha_0(t)] &= \ln\left(1 - \frac{w}{R_{\mp}} \sqrt{\frac{1}{\lambda uv}}\right) + \left(\frac{2[\alpha_0(t) - 1/2]^2\pi^2}{(R_{\mp} - 1/2)^3}\right) D(x_1, x_2, \beta) \\ &= 0, \end{aligned} \quad (8.25)$$

where $D(x_1, x_2, \beta)$ is given by (8.17). This yields the maximal free energy

$$f[\alpha_0(t)] = \frac{1}{2} \ln(\lambda uv) + \frac{2w}{3\pi} \left(\frac{1}{\lambda uv}\right)^{3/4} \sqrt{\frac{uv(1 - \lambda)}{2(2w + u + v - 2\sqrt{uv\lambda})}} t^{3/2}, \quad (8.26)$$

which reflects the proper $\{u, v\}$ symmetry. Results (8.20), (8.22), (8.24) and (8.26) now confirm (8.18). In writing down (8.20), (8.22), (8.24) and (8.26), we have used the respective critical conditions to simplify the expressions.

9 Summary

We have solved the problem of interacting dimers on the honeycomb lattice by solving the equivalent five-vertex model using the method of Bethe ansatz. The free energy is given by (5.11) and the maximal free energy by (5.12) with

Γ_0 , the contour of integrations, subject to constraints (5.13) and (5.15). Phase transitions are then associated with contours either just emerging or completing a closed loop. This leads to the determination of the phase boundaries (7.6), (7.11), (7.12), (7.13) and (7.18), and the phase diagrams shown in Fig. 9. We find the occurrence of a new frozen ordered phase for attractive dimer interactions, and a new first-order line ending at a tricritical point for repulsive dimer interactions. We also find, at $\alpha = 1$, Γ_0 consist of one loop for $|\beta| < 1$ and two loops for $|\beta| > 1$ with the outer loop residing in the infinite regime. But in the latter case Γ_0 can always be deformed into a single loop in computations of the free energy and its derivative with respect to α , much simplifying the algebra. At $\alpha = 1/2$, Γ_0 is found to be the outer loop of two loops, both of which in the finite regime, and this occurs only for $\beta < -4$. We have also evaluated the free energy in perturbative expansions near the phase boundary. This leads to the determination of the critical behavior in the disorder regime with the specific heat exponent $\alpha = 1/2$.

Acknowledgements

One of us (FYW) would like to thank R. J. Baxter for a useful conversation; DK would like to thank M. den Nijs for comments and support during his visit to University of Washington. Work by HYH and FYW is supported in part by NSF grants DMR-9313648 and INT-9207261, and work by DK is supported in part by KOSEF through CTP, by MOE of Korea and by NSF grant DMR-9205125.

References

- [1] P. W. Kasteleyn, *Physica* 27 (1961) 1209.
- [2] M. E. Fisher, *Phys. Rev.* 124 (1961) 1664.
- [3] P. W. Kasteleyn, *J. Math. Phys.* 4 (1963) 287.
- [4] F. Y. Wu, *Phys. Rev.* 168 (1968) 539.
- [5] F. Y. Wu, *Phys. Rev. Lett.* 18 (1967) 605.
- [6] V. L. Pokrovsky and A. L. Talapov, *Phys. Rev. Lett.* 42 (1979) 65.
- [7] J. D. Noh and D. Kim, *Phys. Rev. E* 49 (1994) 1943.
- [8] C. Fan and F. Y. Wu, *Phys. Rev. Phys. Rev. B* 2 (1970) 723.
- [9] B. Sutherland and C. N. Yang, *Phys. Rev. Lett.* 19 (1967) 588.
- [10] I. M. Nolden, *J. Stat. Phys.* 67 (1992) 155.
- [11] D. J. Bukman and J. D. Shore, *J. Stat. Phys.* 78 (1995) 1277.
- [12] J. D. Shore and D. J. Bukman, *Phys. Rev. Lett.* 72 (1994) 604.
- [13] M. Gulácsi, H. V. Beijeren, and A. C. Levi, *Phys. Rev. E* 47 (1993) 2473.
- [14] E. H. Lieb, *Phys. Rev. Lett.* 18 (1967) 692.
- [15] E. H. Lieb and F. Y. Wu, in *Phase Transitions and Critical Phenomena*,
Eds. C. Domb and M. S. Green, vol. 1 (Academic Press, New York 1972).
- [16] M. Gaudin, *La fonction d'onde de Bethe* (Masson, Paris 1983).
- [17] J. D. Noh and D. Kim, unpublished.

Figure captions

Fig. 1. The honeycomb lattice drawn as a brick-wall lattice showing relative positionings of the u , v , and w dimers. The dotted boxes correspond to vertices of the square lattice.

Fig. 2. The six vertex model and the associated weights.

Fig. 3. The four possible ordered states. (a) The U phase with $n = 0$ or $\alpha = 0$ and u dominating. (b) The V phase with $n = N$ or $\alpha = 1$ and v dominating. (c) The W phase with $n = N$ or $\alpha = 1$ and w dominating. (d) The Λ phase with $n = N/2$ or $\alpha = 1/2$ and λ dominating.

Fig. 4. The maximal contour (heavy curve) for noninteracting dimers.

Fig. 5. Possible contours and the corresponding solutions of (5.4) for $\beta > 0$. (a) $d > d_c$. (b) $d = d_c$. (c) $d < d_c$.

Fig. 6. Possible contours and the corresponding solutions of (5.4) for $\beta < 0$. (a) $d > d_c$. (b) $d = d_c$. (c) $d < d_c$.

Fig. 7. Phase diagrams for fixed λ . (a) $\lambda = 1$, the noninteracting case. (b) $\lambda > 1$, the case of attractive interactions between u , v dimers. A new ordered phase Λ arises for $\beta < -4$, or $v/w > 4/(\lambda - 1)$. (c) $\lambda < 1$, the case of repulsive interactions between u and v dimers. The U and V regimes share a first-order boundary denoted by the heavy line, the circle denotes a tricritical point.

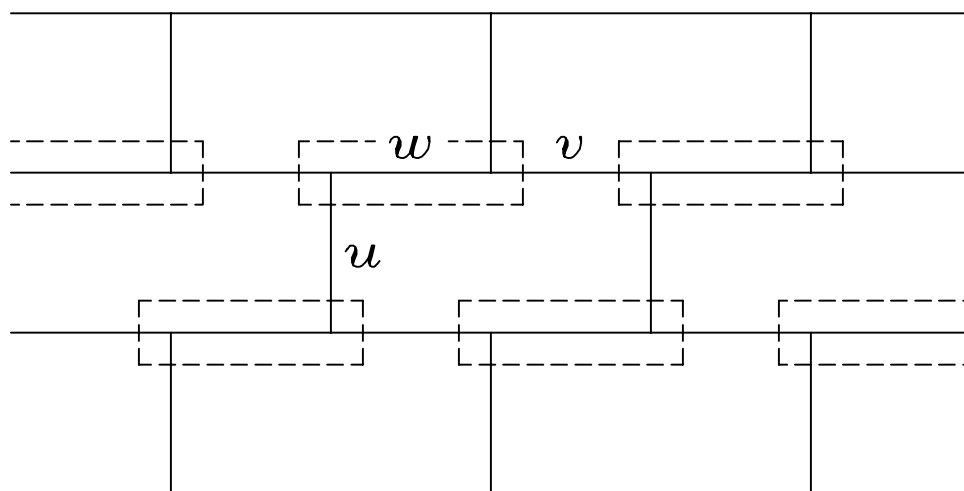


Fig. 1

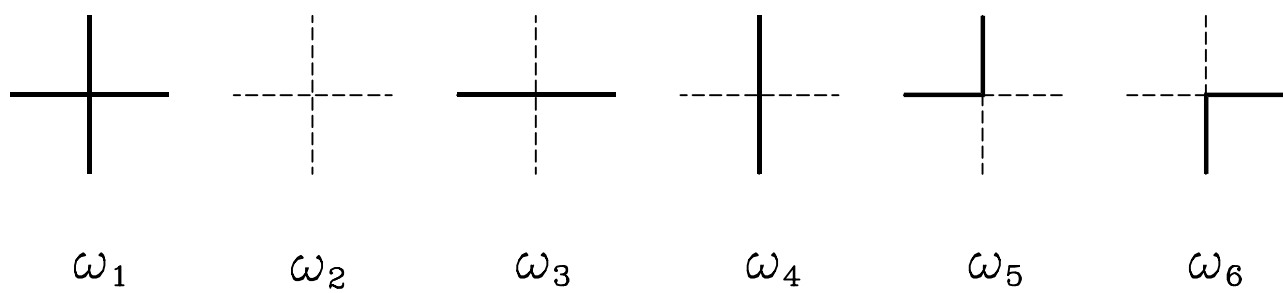
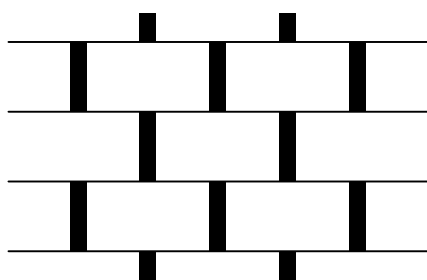
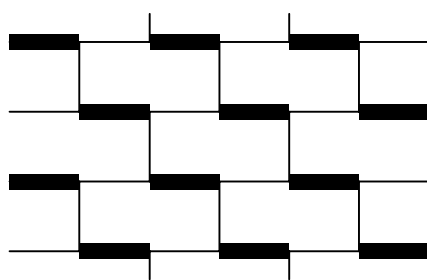


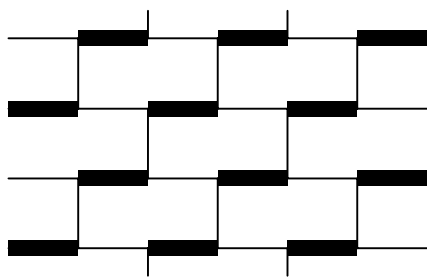
Fig. 2



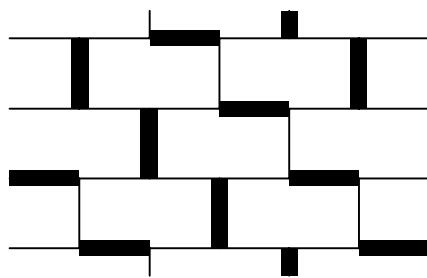
(a)



(b)



(c)



(d)

Fig. 3

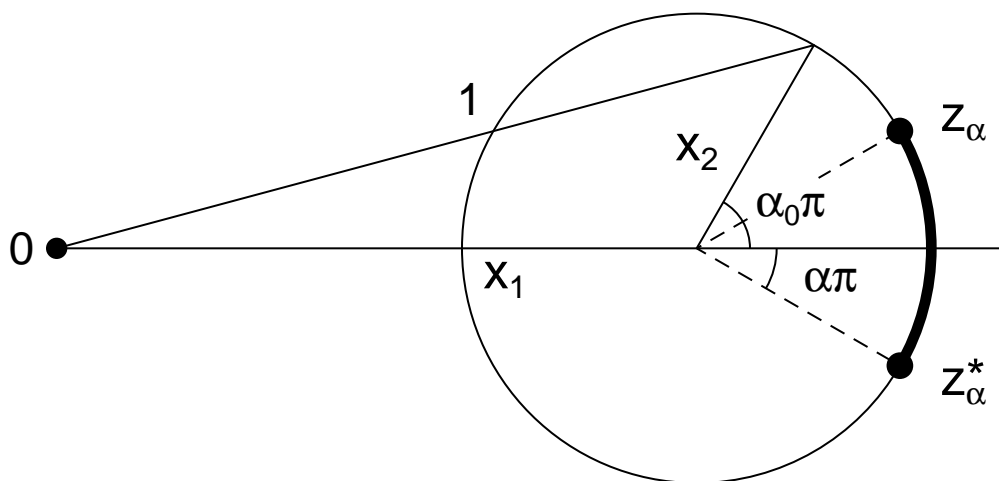
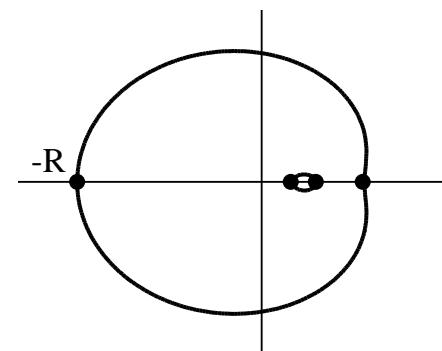
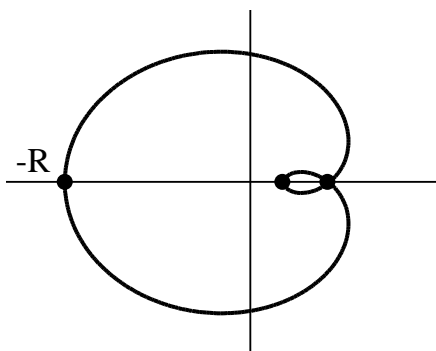
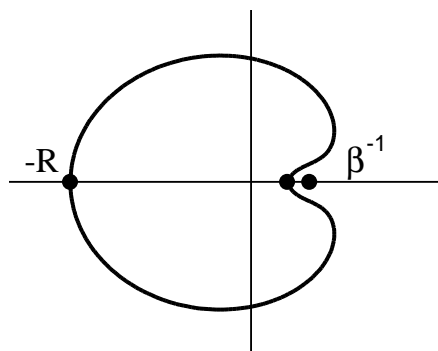
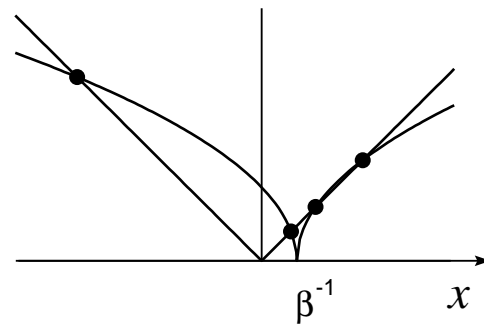
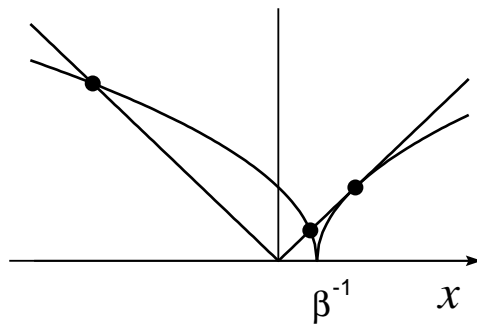
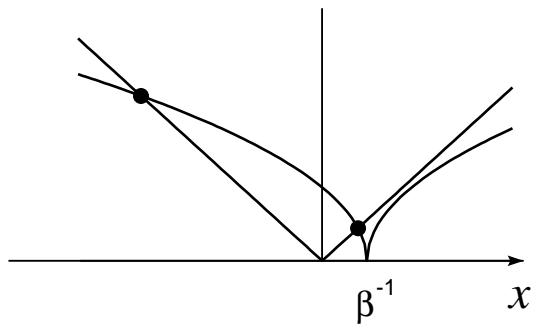


Fig. 4

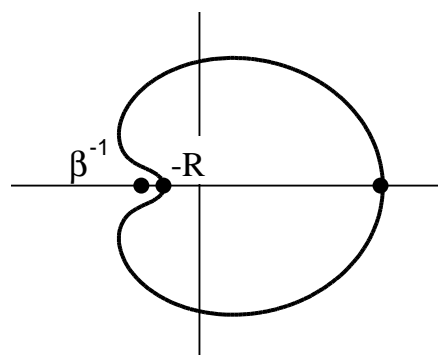


(a)

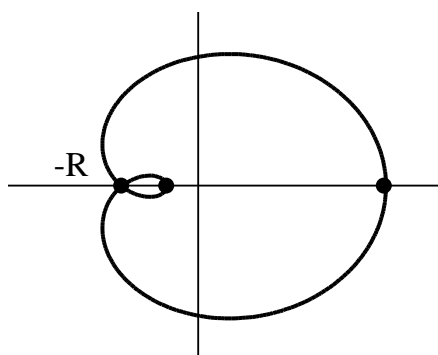
(b)

(c)

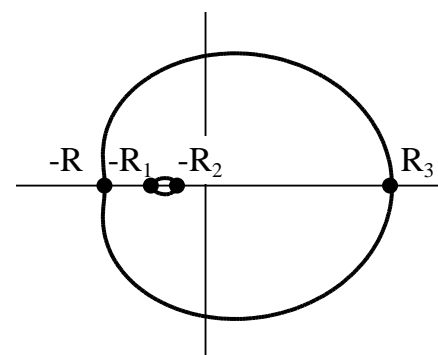
Fig. 5



(a)

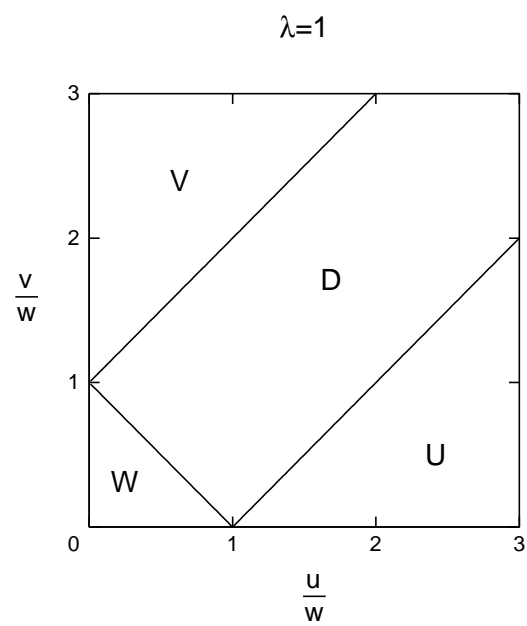


(b)

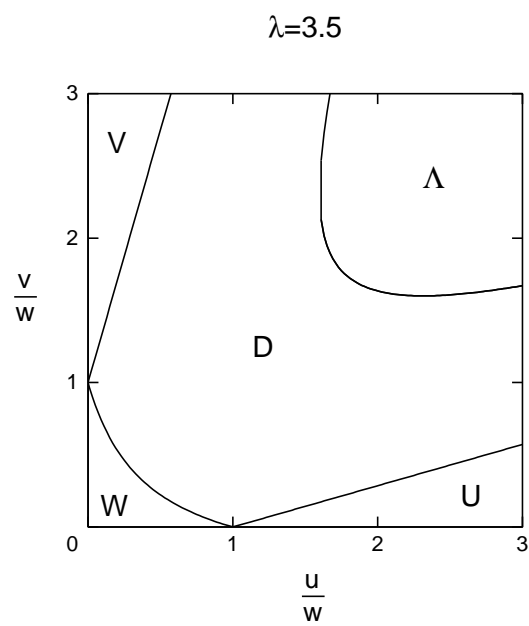


(c)

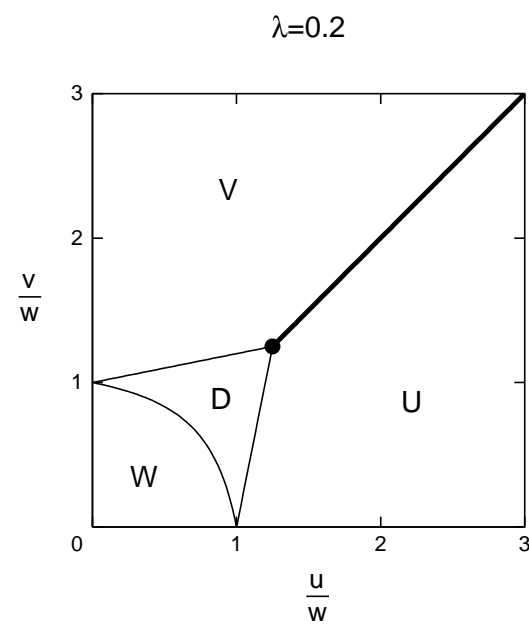
Fig. 6



(a)



(b)



(c)

Fig. 7